Design and Fabrication of Flexure Plate Wave Micro- Sensors Using Lead Zirconium Titanate Thin Films

Jyh-Cheng Yu
Department of Mechanical and Automation Engineering
National Kaohsiung First University of Science and Technology
2, Juoyue Rd., Nantz District, Kaohsiung 811, TAIWAN, ROC.
jcyu@ccms.nkfust.edu.tw

Abstract

This study addresses design, fabrication and possible applications of a flexure plate wave (FPW) resonator using sol-gel-derived lead zirconate titanate (PZT) thin films. Both delay-line and resonator designs are presented, which adopt a two-port structure on a composite membrane of PZT and SiN_x. The asymptotic expression for the phase velocity is applied to derive the sensitivities of the device to pressure, additive mass, and liquid loading. Multiple coatings of sol-gel-derived PZT films are employed because of the cost advantage and the strong electromechanical coupling effect over other piezoelectric films. Fabrication issues such as thermal annealing and poling of PZT thin films are discussed. Experiments show that the frequency and phase angle deviations are linearly related to external disturbances including pressure and additive mass, and demonstrate feasibility of the proposed sensor applications.

1. Introduction

Acoustic wave devices have been popular in signal processing such as filter applications. Because the phase velocity and the attenuation of acoustic waves propagating in the substrate are sensitive to the surface state of the substrate, acoustic wave devices have drawn increasing attention in the areas of mechanical and biochemical sensing[1]. External disturbances such as temperature, pressure[9], additive mass, and viscosity can be measured via deviations of resonance frequency, phase angles, and insertion loss.

The phase velocity of Lamb waves, unlike the velocity of surface acoustic wave (SAW), can be manipulated by selecting proper thickness of the propagating plate. The anti-symmetric zero mode of Lamb wave, A_0, also called the "flexural plate wave" (FPW), propagates on a thin plate with a thickness of 5% or less of the acoustic wavelength, which can be designed to have a phase velocity lower than the velocity of sound in the loading liquid. A thinner plate increases sensor sensitivity. Also, a slow mode of propagation will reduce the radiation energy loss and make FPW devices effective in liquid sensing.

Acoustic wave devices can be applied to biosensing when the sensing area of a delay line is coated with a bio-sensitized film. Pyun etc. [2] deposited an immunoaffinity layer on the membrane of the FPW device to detect Escherichia Coli (E. Coli). The gravimetric detection limit is less than 6 (ng) at a 32 (μm) thick sensitive layer in aqueous media. Some recognize the sensitivity between the velocity of SH-SAW and the pH value of the loading liquid as many bacteria contain urease and generate ammonia that will change the pH value of the solution [3]. Campitelli etc. [4], on the other way, fixed Protein A on a SH-SAW device to detect the concentration of Immunoglobulin G (IgG) by the selective bonding between IgG and Protein A.

Lamb waves are most readily excited and detected using interdigital transducers (IDTs) [5] on a thin piezoelectric plate that is fabricated by the etching of a bulk substrate. Reflecting gratings are added to the FPW devices, as was first reported by Joshi [6], using a Y-X lithium niobate plate to increase the differentiability and the sensitivity of the resonant frequency shift. Piezoelectric thin films have the cost advantage over crystal materials. Most Lamb wave devices of piezoelectric thin films employ zinc oxide (ZnO) [7][8] and aluminum nitride (AlN) [9]. The application of Lead Zirconate Titanates (PZT) thin films is very promising because the electromechanical coupling coefficient (K^2) of is three to nine times over AlN and ZnO, which can greatly improve the sensitivity of sensing devices.

Also, sol-gel deposition is promising because its need for a deposition facility is much less expensive than sputtering and chemical vapor deposition (CVD). Typical sol-gel processes include the preparation of precursor, spin coating and heat

treatment. However, the polycrystalline structure of PZT and the high temperature of the annealing process may cause the cracking and diffusion of structure layers. The deposition of buffer layers, such as LSMO, between the PZT thin film and the structure layers can improve the piezoelectric characteristics, fatigue resistance and ferroelectricity, and reduce leaking current [10].

Although many studies have addressed possible applications of FPW devices, few works analyze sensing selectivity among the mass, tensile stress and viscosity effects, and practical issues that are raised in sensor fabrication and measurement. This investigation will present the design and the fabrication of FPW sensors using sol-gel-derived PZT on silicon nitride and silicon membrane. Sensor applications in liquid density, biological, and pressure sensing will be discussed. Fabrication issues such as material structure and process parameters will also be investigated.

2. Design of FPW Sensors

The proposed FPW sensors utilize a two-port IDT on a composite membrane that comprises piezoelectric layers, a buffer layer and a silicon nitride and/or silicon supporting membrane. Reflectors design can be added to convert the delay-line device to a resonator design (Figure 1). The thickness of the composite membrane is suggested to be 5% or less of the acoustic wavelength λ to excite the lowest mode of the flexural plate wave. For fluid and biosensing applications, the phase velocity of the acoustic wave must be smaller than the velocity of sound in water to reduce the radiation energy loss. Other design parameters are determined by the tradeoff between the device size and sensitivity. An exemplar device assumes 20 pairs of electrodes in both IDTs, 50 wavelength, λ, of overlap length of IDT, and a separation of 10λ between the IDTs.

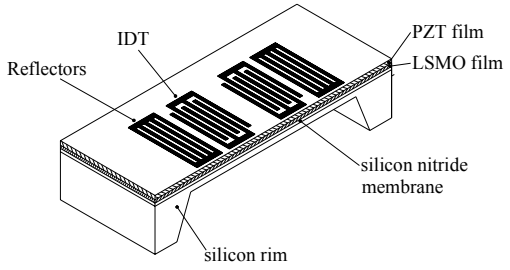

Figure 1 Schematic View of FPW resonators

The design of the reflecting grating is based on a two-port SAW resonator over a bulk PZT that is modeled using COM theory [11][13]. If absorbers are applied to the outside of both reflection gratings; there will be no incident acoustic wave from the outsides of reflective gratings. The spacing between the gratings and the adjacent IDTs is designed to be $(1/8+n/2)\lambda$ to produce a sharp resonant peak. The derived reflector design is applied to the FPW device to increase the differentiability of the frequency deviation associated with disturbing measurands.

3. Sensing Mechanism of FPW Device

3.1. Estimation of phase velocity

The velocity of Lamb wave is determined by the thickness, the mechanical properties, and the boundary the conditions of the conducting composite plate. Therefore, the thin plate can serve as a transducer. The phase velocity of the thin-plate regime can be well approximated by the simple asymptotic expression [12]:

$$v_P = \left(\frac{T_x + B}{M} \right)^{1/2} \tag{1}$$

where B is the bending stiffness of a homogeneous, elastically isotropic plate, T_x is the component of in-plane tension in the propagation direction, and M is the mass per unit area of the plate. For an A_0 Lamb wave in a tension-free plate, the bending stiffness takes the from

$$B = \left(\frac{\lambda}{2\pi} \right)^2 \frac{E' d^3}{12} \tag{2}$$

E' is the effective Young's modulus:

$$E' = \frac{E}{1 - v^2} \tag{3}$$

where E is the Young's modulus and v is the Poisson's ratio of the material.

3.2. Pressure detection

For a square membrane structure, the membrane stresses will be in proportional to applied pressure:

$$(\sigma_x)_{\max} = 0.31 p \frac{a^2}{h^2} \tag{4}$$

where p is the applied pressure, a is the membrane side length, and h is the membrane thickness. The deviation ratio of the phase velocity is as follows:

$$\frac{\Delta v_p}{v_p} = \frac{\Delta f}{f} = s_T \times T_x = \frac{T_x}{2(T_x + B)} \tag{5}$$

The phase velocity is in proportional to the resonant frequency. Therefore, if T_x is much smaller than the bending stiffness, B, of the propagating plate, the deviation ratio of resonant frequency will be linearly related to the applied pressure. However, the deflection of membrane will affect the period of IDT in a nonlinear fashion which will affect the sensor linearity.

3.3. Gravimetric detection of added mass in contact with liquid

When the device is in contact with liquid, additional stiffness effect is introduced by the weight of the liquid and additional mass associated with the

agitation and viscosity damping of the liquid. The phase velocity of the plate regime under tensile stress and liquid loading can be well approximated, as follows [12].

$$v_P = \left(\frac{T_x + B}{M + \rho_F \delta_E + M_\eta} \right)^{1/2} \quad (6)$$

where T_x is stiffness increase due to liquid preesure, $\rho_F \delta_E$ is the mass effect, δ_E is the evanescent decay length, ρ_F is the density of the fluid, and M_η is the viscosity effect.

Equation (7) gives the evanescent decay length, and can be further simplified if the phase velocity is much less than the velocity of sound in the contact liquid.

$$\delta_E = \left(\frac{\lambda}{2\pi} \right) \left[\left(1 - \frac{v_P}{v_F} \right)^2 \right]^{-1/2} \approx \left(\frac{\lambda}{2\pi} \right) \quad (7)$$

The viscosity effect is the product of the liquid density and the viscous decay length:

$$M_\eta = \frac{\rho_F \delta_V}{2} \quad (8)$$

where $\delta_V = \left(\frac{2\eta}{\omega \rho_F} \right)^{1/2}$ is the viscous decay length, ω is the operating angular frequency, and η is the shear viscosity.

3.3.1. *Loading of low-viscosity liquids*

In Eq.(6), the viscosity effect for a low-viscosity liquid is negligible and the phase velocity is influenced solely by the mass effect ($\rho_F \delta_E$) that is determined by the evanescent decay length. However, if the loading liquid is a small droplet on the thin plate and the contacting surface is not hydrophilic, then the droplet does not spread out uniformly but remains hemispherical, as displayed in Figure 2.

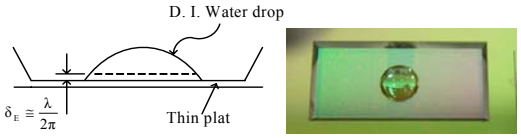

Figure 2 Liquid droplet on the FPW device
(a) Schematic cross section (b) Photo using digital camera

Since only the evanescent decay length of the loading droplet contributes to the mass loading effect and the shape of the droplet cannot be accurately controlled, the change in the phase velocity is normally not proportional to the number of liquid droplets. Hence, the liquid is suggested to fill up the cavity if the device is used to detect the mass effect due to liquid contact. The liquid density solely determines liquid loading as long as the filled liquid level exceeds the evanescent decay length.

The weight of the liquid introduces tensile stress to the membrane, resulting in the deviation of the phase velocity. The sensitivities of the perturbation of the phase velocity to mass and tension are as follows.

$$\frac{\Delta v_p}{v_p} = s_m \times \rho_F + s_T \times T_x \quad (9)$$

where $s_m = -\frac{\delta_E}{2(M + \rho_F \delta_E)}$ and $s_T = \frac{1}{2(T_x + B)}$

The calculated phase velocity of the composite membrane in air is approximately 235 m·s^{-1} which is much less than the speed of sound in water, 1482 (m·s^{-1}). The stiffness of the membrane is estimated using composite plate theory. The calculated sensitivities in the case considered herein are s_m = -2.78 m^2/N and s_T =7.69 × 10^{-5} m/N. If 5 mg of water is loaded on the cavity, the estimated frequency deviation due to the mass loading of water is about -0.94 MHz and the frequency deviation due to the tensile effect is only +1.24 KHz. The tension effect due to the liquid pressure is negligible in comparison with the mass loading effect.

3.3.2. *Loading of viscous liquids*

Equation (6) demonstrates that the fluid density (ρ_F) and shear viscosity (η) of the loading liquid affect the phase velocity of FPW. However, the contributions of liquid density and viscosity to the velocity perturbations cannot be distinguished because the density and the viscosity are coupled in the viscosity effect, as revealed by Eq. (8). Restated, the liquid viscosity cannot be determined by the frequency shift. Hence, the proposed device is unsuitable for measuring the density and viscosity of viscous liquids only from the resonant frequency deviation.

3.3.3. *Bio-sensing Applications*

The device can be applied to a biosensor that may detect the adsorption or attachment of a layer of particular molecules on the sensing region. The phase velocity of the device can be expressed as below:

$$v_P \cong \left(\frac{T_x + B}{M + \rho_F \delta_E + M_\eta + m_{sorptive} + \Delta m} \right)^{1/2} \quad (10)$$

where $m_{sorptive}$ is the mass per unit area of any selective biological or chemically sorptive layer, and Δm is the detectable added mass per unit area. In this study, $m_{sorptive}$ and Δm can be considered as the antibody layer and the locked-in antigen.

Equation (10) shows that the phase velocity of FPW biosensors will be influenced by the coupling effects of (1) the mass effect ($\rho_F \delta_E$) and viscosity effect M_η caused by the loading liquid, (2) the added mass effect (Δm) due to the absorbed antigen, and (3) the tension effect (T_x) caused by the liquid pressure.

$$\frac{\Delta v_p}{v_p} = s_g \times (\rho_F \delta_E + M_\eta + m_{sorptive} + \Delta m) + s_T \times T_x \quad (11)$$

This study proposes the sensor design consisted of two Lamb wave devices as illustrated in Figure 3. The first one is applied to detect external perturbation and the other is filled with the reference solution. Same amount of liquid are loaded on both devices. Here, the comparison of the two devices can isolate the effect of added mass due to antigen bonding and compensates unnecessary perturbation.

3.4. Estimated sensitivity and the phase velocity of the device

Assume the material structure of the proposed FPW device is assumed to be Pt (0.15μm) / Ti (0.02μm) / PZT (1μm) / LSMO (0.1μm) / SiN_x (1.2μm). The PZT properties are assumed from those of the bulk material. The material properties of LSMO are unavailable and assumed to be the same as that of the PZT film. The mass effect of the Pt and the Ti are negligible. Using the composite plate theory, the resonant frequency of the device in air is f_{air} = 5.88 MHz at a wavelength of 40 μm.

For such a device the gravimetric sensitivity is

$$s_g = -\frac{1}{2\left(M + \rho_F \delta_E + M_\eta + m_{sorptive}\right)} \quad (12)$$

We then find that the minimum detectable added mass, $\Delta m_{min,}$ in this fluid-loaded case with a sorptive film is just

$$\Delta m_{\min} = \frac{1}{s_g}\left(\frac{\Delta f_{\min}}{f}\right) \quad (13)$$

where Δf_{min} is the minimum significant frequency shift. Equation (12) shows that the unit membrane mass and the liquid loading parts has a great influence on the sensitivity. Since $\delta_E = \lambda/2\pi$, a smaller wavelength and a thinner membrane can increase s_g in bio-sensing

Assume the viscosity effect, and the weight of the sensitized film and the IDT electrodes are negligible. If the minimum differentiable frequency shift is 100 (Hz), using eq. (13), we can estimate the minimum mass change, Δm_{min} could be detected and examined for the current sensor is approximately $8*10^{-2}$ ($\mu g/cm^2$). The differentiable mass can be smaller if the resolution of frequency deviation can be further decreased.

4. Device Fabrication

4.1. Fabrication Procedure

Figure 4 presents the procedure for fabricating the FPW resonator with a piezoelectric layer coating, silicon etching and the lift-off of IDT. The material system of the resonator is assumed Pt/Ti/PZT/LSMO/SiN_x. The LSMO and the PZT thin films were multiple-coated using sol-gel procedures. The electrodes of the IDT were deposited using E-beam PVD and patterned with period of 40 μm using lift-off. The back cavity was then patterned on SiN_x using RIE. Finally, the membrane cavity of the device was fabricated using KOH anisotropic etching (30ºC, 80%). The final composite membrane comprised 1.2 μm silicon nitride and 1.1 μm PZT layers, and the size of the membrane was approximately 4.2 × 2.7mm. If the device is applied to bio-sensing, the backside of the membrane is deposited Cr and Au as adhesion layers to coat the bio-sensitized film.

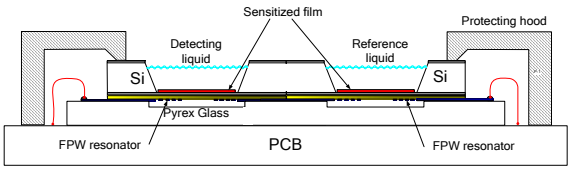

Figure 3 Schematic design of FPW biosensor

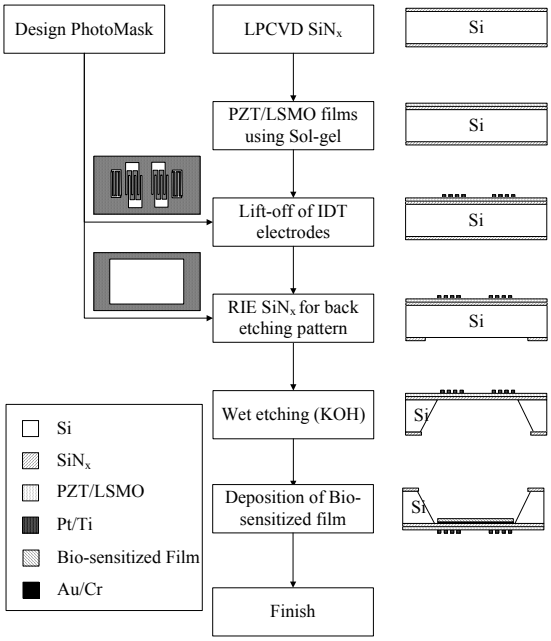

Figure 4 Fabrication procedure of the bio-sensor using FPW resonator

4.2. Sol-Gel Deposition of PZT

Sol-gel derived PZT thin films require heat treatment to be transformed into polycrystalline piezoelectric layers. Furnace heating is performed herein this study. Increasing the heat treatment temperature may improve the material characteristics of PZT, but severe thermal stresses may crack the film because of thermal stresses and interface incompatibility among constituent layers. The experimental results show that the heat treatment of PZT films at 650°C yields satisfactory perovskite structures without a pyrochlore phase.

LSMO coating is used as a buffer layer between PZT and SiN_x; it enhances the piezoelectric characteristics and prevents possible cracking of PZT. Experiments show that the LSMO buffer layer not only increases residual polarization but also reduces the polarization decay due to fatigue loading that is very important for resonant devices.

4.3. Parallel poling of the PZT films with IDT

Because PZT is polycrystalline, polarization using DC poling will increase the net capacitance of the transducer. There are three main factors influencing the poling result including poling time, poling voltage, and substrate temperature. The poling level can be measured by the capacitance (C_s) using LCR meters. The IDT is used as poling electrodes directly. We first vary the poling voltage from 10(V) to 50(V) at substrate temperature of 250(°C) for three hours. The capacitance increases significantly with the applied poling voltage, and saturates when the applied voltage exceeds 40(V). Next, the poling voltage is set at 40 V for 3 hours when the heating temperature varies from room temperature to 300(°C) (Figure 5). Again, the capacitance increase saturates when the poling temperature reaches 250(°C). Therefore, the poling conditions of 40 V for 3 hours with substrate heated at 250(°C) are suggested.

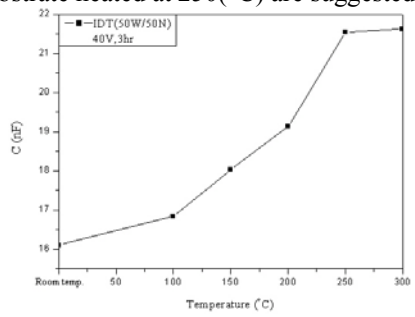

Figure 5 Relation between the IDT capacitance and the substrate temperature at DC poling of 40V for 3hr.

5. Experimental Results and Discussion

5.1. FPW delay line and FPW resonator signals

Figure 7 plots the frequency responses of the FPW delay line and the FPW resonator measured using a network analyzer (HP8753 ES). The resonant frequency without liquid loading is 5.53 MHz, which is quite close to the theoretical estimate of 5.88 MHz. The difference may follow from the use of the bulk material properties in the theoretical estimate since the PZT film properties are unknown. The resonator has a more differentiable resonant signal than the delay line design, although no sharp peak is observed, perhaps because PZT has a polycrystalline structure[13].

5.2. The deposition of the bio-sensitized film

The bio-sensitized film is deposited on the cavity side of the membrane. The first step is to deposit A Au/Ti adhesion layer is used between the antibody layer and the SiN membrane. The depositing result is examined using immuofluorescence as illustrated in Figure 6. Fluorescent dye (FITC) are first conjugated to antibody. When the antibodies is successfully fixed on the membrane, luminous points will be observed under argon laser light source.

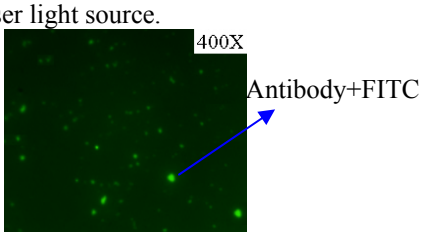

Figure 6 Coating of the bio-sensitized film

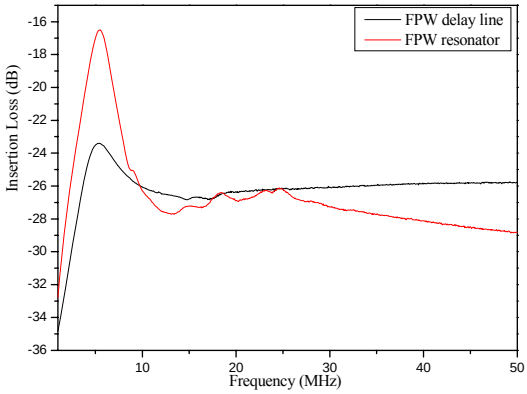

Figure 7 S_{21} frequency response of the FPW devices

5.3. Pressure sensing using FPW delayline

The period of the FPW delay line is 100 μm. For fracture consideration, the membrane consists of 30 μm silicon. The material system of the delayline is Pt/Ti/PZT/LSMO/SiO_2 (1.8 μm) /Si. Here the phase deviation is recorded when the pressure is applied as shown in Figure 8. The Phase angle decrease linearly with the applied pressure.

5.4. Liquid sensing using FPW resonator

Three low-viscosity liquids, DI Water (1 g/cm^3), IPA (0.787 g/cm^3) and saline solution (1.2 g/cm^3), are applied to the resonator. The viscosity effect is negligible compared with the mass effect. Figure 9 presents the density sensitivity to the resonant frequency. The theoretical sensitivity for low-viscosity liquids is -0.848 (Mhz/g·cm^{-3}). The resonant frequency and the liquid density are strongly linearly correlated despite a static difference between the theoretical and experimental curves, which demonstrates the feasibility of density sensing. The static difference may be due to the use of bulk

material properties in the theoretical estimates and liquid damping which was presumed negligible [14].

However, theoretical analysis indicates that fluid density and shear viscosity of a high-viscosity liquid affect the phase velocity of FPW. The contributions of liquid density and viscosity to velocity perturbations cannot be distinguished because they are coupled in the viscosity effect. Herein, two liquids, glycerol with a viscosity of 934×10^{-3} (Ns/m^2) is compared with a low-viscosity saline solution of the same density (1.2 g/cm^3) to investigate the viscosity effect. Table 1 shows that glycerol loading introduces an additional frequency deviation than the saline solution of the same density. Also, the viscosity effect of glycerol causes greater dampening than does that of the saline solution and increases the insertion loss.

6. Conclusions

Although the polycrystalline structure of PZT may obscure the resonant peak of the frequency response, the peak is sufficient to differentiate the frequency deviation due to liquid loading. The experiments show that proper poling will increase the sensing sensitivity. Possible application in pressure sensing is validated. Liquid loading increases the insertion loss and reduces the resonant frequency in a manner consistent with theoretical prediction. For a low-viscosity liquid, the deviation of resonant frequency can determine the liquid density. As to the applications of high-viscosity liquids, the proposed device cannot differentiate the velocity perturbations associated with liquid density and viscosity, which restrains the applications. In case of bio-sensing, dual sensors can be applied to isolate the additive mass due to antigen sensing. The estimated sensitivity and the fabrication status check demonstrate the application feasibility.

7. References

[1]. Vellekoop, M. J., Acoustic wave sensors and their technology, *Ultrasonic*, Vol.36, pp. 7-14, 1998

[2]. Pyun, J.C., Beutel, H., Meyer, J.-U., and Ruf, H.H. "Development of a biosensor for E. coli based on a flexural plate wave (FPW) transducer", *Biosensors & Bioelectronics*, v 13, n 7-8, pp. 839-845, Oct 1, 1998.

[3]. Kondoh, J, Matsui, Y, and Shiokawa, S., "SH-SAW biosensor based on pH change", *IEEE Ultrasonics Symposium Proceedings*. vol.1, pp.337-340, 1993.

[4]. Campitelli, A., Wlodarski, W., Hoummady, M., and Sawyer, W., "Shear horizontal surface acoustic wave based immunosensing system", *Solid State Sensors and Actuators. TRANSDUCERS '97* Chicago., 1997.

[5]. White, R. M. and Voltmer, F. M. "Direct piezoelectric coupling to surface elastic waves", *Appl. Phys. Lett*., Vlo. 7, pp. 314-316, 1965.

[6]. Joshi, S. G. and Zaitsev, B. D., Reflection of ultrasonic Lamb waves propagating in thin piezoelectric plates, *Ultrasonics Symposium*, pp.423-426, 1998.

[7]. Vellekoop, M.J., Lubking, G.W., Sarro, P.M., and Venema, A. "Evaluation of liquid properties using a silicon lamb wave sensor", *Sensors and Actuators A*, 43, pp.175-180, 1994.

[8]. Wenzel, S. W. and White, R.M., "A Multisensor Employing an Ultrasonic Lamb-Wave Oscillator", *IEEE Transactions on Electron Devices*, Vol.35, No.6, pp.735-743, June 1988.

[9]. Choujaa, A., Tirole, N., Bonjour, C., Martin, G., Hauden, D., Blind, P., Cachard, A., and Pommier, C. "AlN/silicon lamb wave microsensors for pressure and gravimetric measurements", *Sensors and Actuators A*, Vol. 46, pp. 179-182, 1995.

[10]. Chen, M. S., Wu, T. B., Wu, J. M., "Effect of Textured $LaNiO_3$ Electrode on the Fatigue Improvement of $Pb(Zr_{0.53}Ti_{0.47})O_3$ Thin Films", *Appl. Phys. Lett.*, 68[10], pp. 1430-1432, 1996.

[11]. Campbell, C. K., *Surface acoustic wave devices for mobile and wireless Communications*, San Diego: Academic Press, 1998.

[12]. White, R. M. et al., *Acoustic Wave Sensors Theory, Design, and Physico-Chemical Applications*, Academic Press, 1996.

[13]. Yu, J. and Lin, H.Y. (2008) "Liquid Density Sensing Using Resonant Flexural Plate Wave Devices with Sol-Gel PZT Thin Films" *Microsystem Technologies* . Vol. 14, No. 7, pp. 1073-1079.

[14]. Yu, J. and Lin, H.Y. (2007) "The Design of a FPW Resonator using the Composite Membrane of PZT Layer and SiN_x for Liquid Sensing", *Tamkang Journal of Science and Engineering*, Vol. 10, No 2, pp. 163-166.

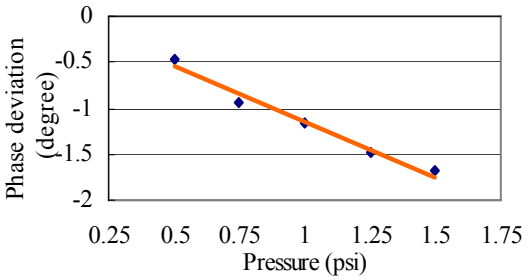

Figure 8 Phase deviation vs. applied pressure

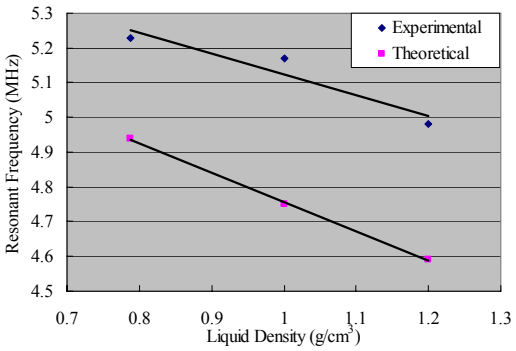

Figure 9 Sensitivity analysis of the resonant frequency and the density of low-viscosity liquids

Table 1 Viscosity effect on the resonant frequency and insertion loss

	Theoretical	Experimental	
	Frequency (MHz)	Frequency (MHz)	Insertion Loss (dB)
Saline solution	4.59	4.98	-33.38
Glycerol	4.49	4.73	-37.04